Universal Digital Sliding Mode Control for DC-DC Converters

Andreas Berger[1], Matteo Agostinelli[2], Robert Priewasser[2], Stefano Marsili[2] and Mario Huemer[1]

[1]Institute of Networked and Embedded Systems
University of Klagenfurt
9020 Klagenfurt, Austria
email: andreas.berger@aau.at

[2]Infineon Technologies Austria AG
9500 Villach, Austria
email: stefano.marsili@infineon.com

Abstract

Recent research in the field of DC-DC converters revealed a huge potential for the nonlinear control technique Sliding Mode Control (SMC). Various state-of-the-art publications, e.g. [1]–[4], only consider an analog controller implementation, since a feasible digital implementation is not straightforward. In this paper, a digital sliding mode controller for DC-DC converters is presented. In order to be applicable for different converter topologies and operation modes, information of the inductor current is used as an input for control. Hence, the required current has to be sensed or estimated. The digital sliding mode algorithm is implemented in a simulation environment, where the system parameters are chosen to represent a realistic Power Management Unit (PMU) for a mobile device. Results of the simulations are presented for a Buck converter operating in Continuous Conduction Mode (CCM). Based on the simulations it is shown that the proposed digital control algorithm achieves a small voltage ripple in steady-state, and an excellent dynamic performance under different operation conditions.

I. Introduction

The application of digital control algorithms to DC-DC converters is attracting increasing interest in the recent years [5]–[7]. The main reasons for this trend are among others the high flexibility and reusability of digital controllers. Furthermore, they enable the possibility to implement complex control algorithms with reasonable hardware effort. On the other hand, a digital implementation requires an additional Analog-to-Digital Converter (ADC), which has to be considered during the design.

Recent research on DC-DC converters showed a high potential for improving the dynamic performance by applying Sliding Mode Control (SMC) [1]–[3]. This nonlinear control scheme is especially well suited for Variable Structure System (VSS) like DC-DC converters [8]. The main advantage of SMC over common linear control schemes is its high robustness against line, load and parameter variations [4]. Furthermore, the same control structure can be used with the same coefficients when switching between different operation modes and hence transient effects can be avoided. Moreover, the derived approach is applicable for different topologies like Buck, Boost or Buck-Boost converters. A major drawback of this technique is the variable switching frequency, which is undesirable in many applications because of possible problems with Electro-Magnetic Interference (EMI) at adjacent parts of the system.

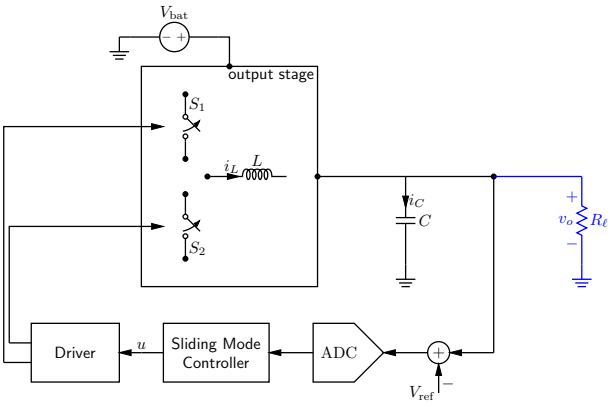

Fig. 1. High-level representation of the system under exam, consisting of a DC-DC converter (e.g. a Buck converter), an ADC, a controller and a driver stage.

In this paper a digital control structure based on the theory of sliding mode control [9]–[11] is presented for a Buck converter operating in Continuous Conduction Mode (CCM). Fig. 1 shows a schematic representation of the investigated system. The conventional sliding mode algorithm has been modified to operate at a constant switching frequency, thus reducing EMI issues of the proposed control structure [12]. It is highlighted that the developed controller represents a unified approach which is not restricted to a Buck converter operating in CCM.

The remainder of this paper is organized as follows: Section II gives an introduction to the theory of sliding mode control and its application to DC-DC converters. The implementation specific issues of the digital sliding mode controller are summarized in Section III. Section IV presents the results of the developed simulation environment and Section V provides a comprehensive summary of the major findings.

II. Sliding mode control

Sliding mode control has been verified to be a very effective control technique for regulating VSSs like DC-DC converters [13]–[15]. On the other hand, SMC has some major drawbacks like the variable switching frequency of a pure sliding mode controller implementation [16]–[18] and the additional need for current sensing or estimation if the control structure is defined for a unified approach. However, this disadvantages can be overcome for certain applications by a digital controller implementation as proposed in this paper.

A. Sliding mode theory

A general mathematical model for a dynamic VSS, including also different types of DC-DC converters [9], is given by

$$\dot{\mathbf{x}} = \mathbf{f}\left(\mathbf{x}, t, u\right), \tag{1}$$

where $\mathbf{x} \in \mathbb{R}^{\mathrm{n}\times 1}$ is the vector of state variables, $t \in \mathbb{R}$ is the time and $u \in \{u^+, u^-\}$ is the actuating signal. The sliding mode controller forces the Representative Point (RP) of the system to hit the sliding surface $\sigma(\mathbf{x}, t) = 0$ in a first step. After this so-called reaching phase, the SMC forces the RP to stay on the sliding surface while concurrently sliding down on the surface until the trajectory reaches the desired equilibrium point. In this second phase, the system is said to be in sliding mode. The control law to achieve this can be written as

$$u = \begin{cases} u^+ & \text{if } \sigma(\mathbf{x}) > 0 \\ u^- & \text{if } \sigma(\mathbf{x}) < 0. \end{cases} \tag{2}$$

Hence, for VSSs the function $\mathbf{f}$ is discontinuous on the sliding surface $\sigma(\mathbf{x}, t) = 0$ and can be expressed as

$$\mathbf{f} = \begin{cases} \mathbf{f}^+(\mathbf{x}, t, u^+) & \text{if } \sigma \to 0^+ \\ \mathbf{f}^-(\mathbf{x}, t, u^-) & \text{if } \sigma \to 0^-, \end{cases} \tag{3}$$

where 0^+ denotes an approaching of 0 from positive values and 0^- from negative values, respectively. During sliding mode operation the dynamic behavior of the system is almost independent of the plant parameters and depends solely on the definition of the sliding function $\sigma(\mathbf{x})$ [10]. An exemplary trajectory of the RP of a system under sliding mode is shown in Fig. 2, where the actuating signal u is defined as $u^- = 1$ and $u^+ = 0$, representing the logical states "*on*" and "*off*" of the investigated system.

The choice of the sliding function is of key importance to ensure that the existence, reaching and stability conditions of the sliding mode controller are fulfilled [9]. The reaching condition ensures that for every possible starting point of the trajectory in the phase plane, the RP is directed towards the sliding surface in finite time. For this purpose, it is sufficient to demonstrate that the steady state RP corresponding to u^+ (u^-) lies in the

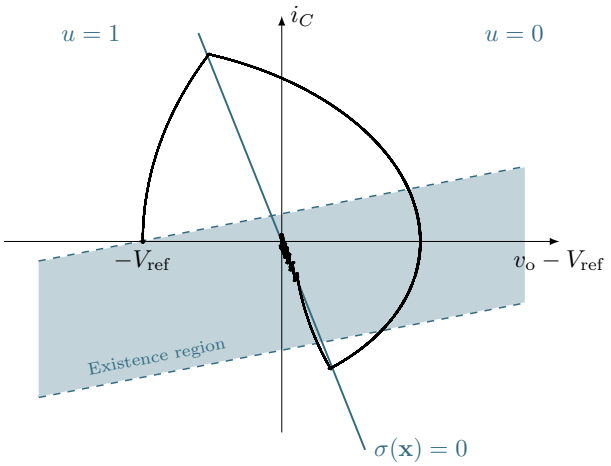

Fig. 2. An example trajectory of a system under sliding mode. In this case, $\sigma(\mathbf{x})$ is a linear combination of the error of the output voltage and the capacitor current of a Buck converter. Note that the equilibrium point is the origin of the phase plane, which yields output voltage regulation $v_o = V_{\mathrm{ref}}$.

portion of the state space relative to u^- (u^+). Therefore, the reaching condition is met if

$$\mathbf{x}^+ \in \sigma(\mathbf{x}) < 0$$
$$\mathbf{x}^- \in \sigma(\mathbf{x}) > 0,$$

where $\mathbf{x}^+$ ($\mathbf{x}^-$) is the steady state RP when the actuating signal $u = u^+$ ($u = u^-$). The existence condition assures that, if the RP is near the sliding surface, the trajectory will be directed towards $\sigma(\mathbf{x}) = 0$. Hence, if the system trajectory approaches the sliding surface from $\sigma(\mathbf{x}) < 0$, $\mathbf{f}^-$ has to be directed towards $\sigma(\mathbf{x}) = 0$, and if it approaches from $\sigma(\mathbf{x}) > 0$, $\mathbf{f}^+$ is steered in direction of $\sigma(\mathbf{x}) = 0$, respectively. To derive the existence condition, a positive definite Lyapunov function candidate $V(x)$ is introduced

$$V(x) = \frac{1}{2}\sigma^{\mathrm{T}}(\mathbf{x})\sigma(\mathbf{x}). \tag{4}$$

The chosen Lyapunov function can be interpreted as the distance to the sliding surface since $\sigma^{\mathrm{T}}(\mathbf{x})\sigma(\mathbf{x}) = \|\sigma(\mathbf{x})\|_2^2$. In order to satisfy the existence condition, the time derivative of $V(x)$ has to be negative definite, given by (5), and thus the distance to $\sigma(\mathbf{x}) = 0$ reduces over time

$$\frac{\mathrm{d}V(x)}{\mathrm{d}t} = \sigma(\mathbf{x})\frac{\mathrm{d}\sigma(\mathbf{x})}{\mathrm{d}t} < 0. \tag{5}$$

For the definition of the sliding function a linear combination of the state variables is chosen, given by

$$\sigma(\mathbf{x}, t) = \mathbf{s}^{\mathrm{T}}\mathbf{x}(t), \tag{6}$$

where $\mathbf{s}^{\mathrm{T}} = [s_1 \ \ldots \ s_n] \in \mathbb{R}^{1\times \mathrm{n}}$ is the vector of coefficients of the sliding function. It can be immediately seen that $V(x)$ is positive definite and (4) results in

$$\begin{cases} \mathbf{s}^T \cdot \mathbf{f} > 0 & \text{if } \sigma < 0 \\ \mathbf{s}^T \cdot \mathbf{f} < 0 & \text{if } \sigma > 0. \end{cases} \tag{7}$$

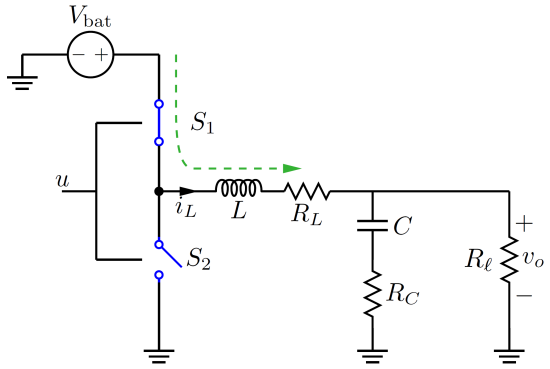

(a) Buck "*on*" configuration ($u = u^-$)

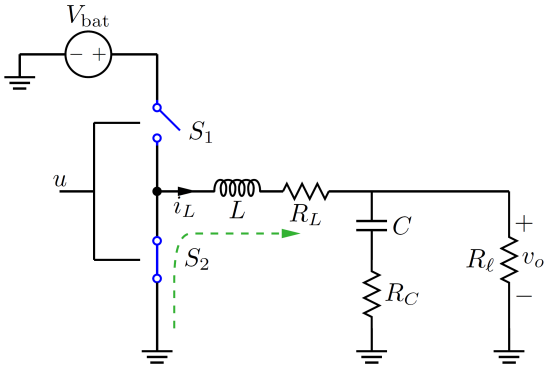

(b) Buck "*off*" configuration ($u = u^+$)

Fig. 3. Buck converter in open-loop configuration, including the most important parasitic components. Subfigure (a) depicts the "*on*" configuration, while subfigure (b) depicts the "*off*" configuration.

Finally, the system stability is guaranteed if the trajectory is directed towards a stable operating point when in sliding mode operation. Stability can be analyzed via the equivalent model of the system under sliding mode.

B. Application to DC-DC converters

Due to their switching nature, DC-DC converters can be considered as VSS [9]. The structure of DC-DC converters is changing over time during operation, according to the value of the input Pulse Width Modulation (PWM) signal u, which is driving the switches of the converter. A schematic representation of the investigated system is shown in Fig. 3.

The definition of the sliding surface $\sigma(\mathbf{x}) = 0$ is of key importance because it directly influences the dynamic behavior of the system [19], as stated previously. Since the derivative of the output voltage v_o is discontinuous for a boost converter, it cannot be included into a general definition of the sliding function, which shall be employed for different converter topologies [11], [13]. Alternatively to the error dynamics, the inductor current is a feasible choice as a state variable of the control system. This allows a general definition of the sliding function with the drawback that the inductor current has to be sensed. Otherwise, i_L needs to be estimated if a pure voltage-mode controller is desired. Hence, the vector of state variables $\mathbf{x}$, applicable for different topologies is defined as

$$\sigma(\mathbf{x}) = \mathbf{s}^T\mathbf{x} = s_1x_1 + s_2x_2 + s_3x_3, \tag{8}$$

$$\mathbf{x} = \begin{bmatrix} x_1 \\ x_2 \\ x_3 \end{bmatrix} = \begin{bmatrix} v_\text{o} - V_\text{ref} \\ i_\text{L} \\ \int (v_\text{o} - V_\text{ref})\text{d}t \end{bmatrix}, \tag{9}$$

where v_o is the sensed output voltage, V_ref is the set point of the output voltage and i_L is the inductor current. The additional integral term is needed to remove the steady-state error, as in general it holds that the average value of the inductor current over a switching period $\langle i_L \rangle_{T_\text{sw}} \neq 0$. By the addition of the integral part, the proposed definition represents a full-order approach for the sliding mode controller, since it has the same order as the system. For ease of calculation, the first coefficient s_1 has been set to 1 in the following analysis, without loss of generality.

C. Application to a Buck converter

In this subsection, the design of the proposed digital sliding mode controller is shown for a Buck converter. Furthermore, the necessary conditions for the choice of the sliding coefficients are derived for this particular case. If the state variable vector $\mathbf{x}$ is defined as in (9), the state-space representation of a Buck converter can be denoted by

$$\dot{\mathbf{x}} = \mathbf{A}\mathbf{x} + \mathbf{B}u + \mathbf{D},$$

$$\mathbf{A} = \begin{pmatrix} -\frac{1}{R_\ell C} & -\frac{1}{C} & 0 \\ -\frac{1}{L} & 0 & 0 \\ 1 & 0 & 0 \end{pmatrix}, \mathbf{B} = \begin{pmatrix} 0 \\ \frac{V_\text{bat}}{L} \\ 0 \end{pmatrix}, \mathbf{D} = \begin{pmatrix} -\frac{V_\text{ref}}{R_\ell C} \\ -\frac{V_\text{ref}}{L} \\ 0 \end{pmatrix},$$

where L and C are the values of the inductance and capacitance of the output filter, V_bat is the input (battery) voltage, and R_ℓ is the load resistance.

To verify the reaching condition, it is sufficient to check, if the steady-state RP corresponding to $u = u^+$ ($v_\text{o} \to 0$) lies in the portion of the state space corresponding to $u = u^-$ ($v_\text{o} \to V_\text{bat}$) and vice versa. For reasonable values of V_bat and V_ref ($V_\text{bat} > V_\text{ref} > 0$) this condition is always fulfilled for the given setup.

In order to meet the existence conditions, the state-space model of the Buck converter is inserted into (7) to obtain

$$\begin{cases} -\frac{1}{C}i_L + s_2\frac{V_\text{bat} - V_\text{ref}}{L} - \frac{V_\text{ref}}{R_\ell C} > 0 & \text{if } \sigma < 0, \\ -\frac{1}{C}i_L - s_2\frac{V_\text{ref}}{L} - \frac{V_\text{ref}}{R_\ell C} < 0 & \text{if } \sigma > 0. \end{cases} \tag{10}$$

The derived existence conditions in (10) form a so-called existence region which bounds the possible values of the sliding coefficients s_i.

The last condition which has to be verified is the stability condition of the system in sliding mode. As soon as the RP reaches the sliding surface, the controller forces the trajectory to stay there, i.e. $\dot{\sigma} = 0$, yielding

$$\frac{\mathrm{d}x_1}{\mathrm{d}t} + s_2 \frac{\mathrm{d}x_2}{\mathrm{d}t} + s_3 x_1 = 0, \tag{11}$$

which can be reduced to a differential equation in x_1 only

$$\frac{\mathrm{d}^2 x_1}{\mathrm{d}t^2} + \frac{1}{C s_2}\left(1 + \frac{s_2}{R_\ell}\right)\frac{\mathrm{d}x_1}{\mathrm{d}t} + \frac{s_3}{C s_2} x_1 = 0. \tag{12}$$

If (12) is a Hurwitz polynomial, the eigenvalues have a negative real part which ensures stability of the system. The values of the components are always positive. Thus, from (12) it can be obtained that in order to meet the stability condition both coefficients s_2 and s_3 have to be positive. The possible choice of the coefficients of the sliding function is bounded by the derived conditions.

III. Digital implementation details

The control structure presented in Sec. II has been implemented in the digital domain. Hence, an ADC is needed to sample the output voltage error, as shown in Fig. 1. For the proposed setup a window flash ADC with a sampling frequency $f_s = 6.25\,\mathrm{MHz}$, corresponding to 4 samples per switching period (at a switching frequency $f_{\mathrm{sw}} = 1.56\,\mathrm{MHz}$), a quantization step size of $10\,\mathrm{mV}$ and a resolution of 4 bits is used to sample the output voltage error. Moreover, a driver stage is needed to generate the driving signals for the power MOSFETs of the output stage. Further details on several implementation issues are examined in the following subsections.

A. Constant switching frequency

A pure sliding mode controller switches at a very high frequency during the sliding phase. This behavior is undesired in most applications because of high switching losses and possible EMI problems. Furthermore, the implemented switches are only able to switch at a certain rate due to physical limitations. Hence, in a practical application, only a so-called quasi sliding mode operation can be achieved, where the switching frequency is constrained to a certain maximum value.

Various constant frequency techniques have been proposed in literature, such as dynamically adapting the amplitude of the hysteresis band [4], or using a PWM-based sliding mode approach [8]. In this paper, a different technique is used: the PWM signal u is set to a logical "*on*" state at every rising edge of a clock signal (running at the desired switching frequency f_{sw}) and reset to "*off*" state, when the sliding function reaches a pre-determined threshold level. Hence, the operation of the converter is synchronized to the clock signal, which sets the switching frequency. To avoid frequency variations due to high load variations, a minimum "on" and "off" time of the PWM signal u is introduced. A schematic representation of the controller is reported in Fig. 4.

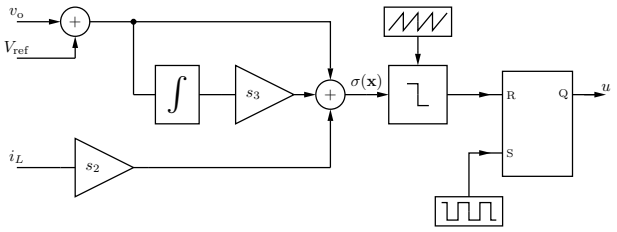

Fig. 4. High-level representation of the sliding surface generation and synchronization to a clock signal.

B. Slope compensation

It is well known from literature that a fixed-frequency current-mode control leads to a static instability if the duty cycle of the PWM actuating signal u exceeds 50% for the case of a Buck converter [20]. Then the PWM signal oscillates between a very large and a very small duty cycle. The result is on average correct, but the voltage and current ripple increases significantly. Since the operating frequency is fixed and current information is used by the controller, the same applies for the proposed sliding mode control structure. To avoid this kind of instability, a ramp has to be added to the definition of the sliding function. The ramp consists of an accumulator which counts up by 1 at the rate of the system clock frequency f_{clk} and resets to 0 at the beginning of every PWM switching period $T_{\mathrm{sw}} = 1/f_{\mathrm{sw}}$. Furthermore, the ramp has to be properly scaled by an additional scaling factor before accumulating to the sliding function. To reduce complexity, the same counter as in the switching period generation process has been used for the generation of the ramp.

C. Sliding surface generation

The overall digital implementation of the sliding surface generation is shown in Fig. 5. In the first branch, the output voltage error $v_o - V_{\mathrm{ref}}$, which is computed by the ADC, is filtered by a first-order low-pass filter to reduce the influence of disturbances on the analog-to-digital conversion. This part is the first term in the sum, forming the sliding function. The first sliding coefficient s_1 is assumed to be 1, without loss of generality. Hence, no gain factor is needed in this branch. The second branch computes the integral of the voltage error and scales the result with the coefficient s_3 before adding it to the sliding sum. The remaining two branches are the inductor current information and the artificial ramp generation. It is worth noting that the coefficients s_i have been chosen such that the scaling can be realized solely by shift operations. This avoids the need for multiplications and hence reduces the overall complexity of the system.

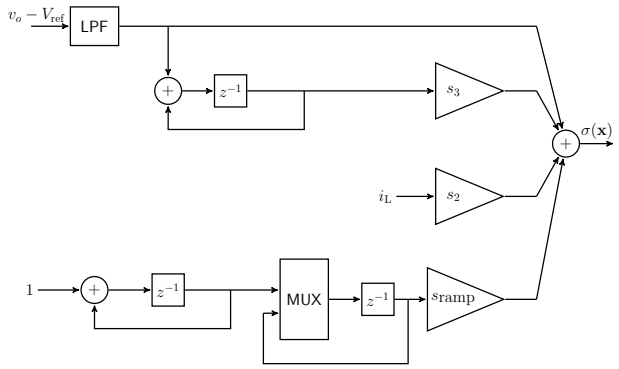

Fig. 5. Digital implementation of the sliding surface computation. The comparator and the flip-flop, as shown in Fig. 4, are omitted in this figure for simplicity.

The operating frequency of the digital core f_{clk} has been set to 100 MHz for the given setup. This defines the maximum possible accuracy of the turn-off slope of the PWM signal. The computed sliding function $\sigma(\mathbf{x})$ is then fed to the input of the comparator shown in Fig. 4, which is updated at the system clock rate f_{clk}. The operating frequency of the digital core has been chosen to be much higher than the switching frequency of the PWM signal driving the Buck converter ($f_{\text{clk}} \gg f_{\text{sw}}$). Hence, the models derived in Sec. II for the analog domain are still valid with very good approximation, and it is not required to discretize the system model. On the other hand, the output voltage error is sampled by the ADC at a lower rate of 6.25 MHz. Thus, the reaction time of the controller to a transient on the output voltage is limited by this rate.

IV. Results

The system has been successfully modeled in a MATLAB/Simulink simulation environment. The system parameters have been chosen to represent a real-life commercial application based on [21], which is a Buck converter for wireless applications. The values of the main system parameters of the converter are reported in Tab. I. The sliding coefficients have been tuned in order to achieve a good dynamic performance with a low steady-state output voltage ripple. The used values of the coefficients are reported in Tab. II.

TABLE I. System parameters

Parameter	Value	Parameter	Value
V_{bat}	3.3 V	R_C	20 mΩ
V_{ref}	1.3 V	R_L	100 mΩ
f_{sw}	1.56 MHz	R_n	100 mΩ
L	4.7 µH	R_p	100 mΩ
C	10 µF	f_{clk}	100 MHz

TABLE II. Controller parameters

Parameter	Value	Parameter	Value
s_1	1	s_3	2^{-4}
s_2	2^5	s_{ramp}	2^8

The dynamic performance of the proposed digital control architecture has been tested by means of simulations during load variations. This is a typical condition in mobile devices, e.g. if a component wakes up from standby mode and hence a step in the required current occurs in a very short time period. Notwithstanding this load variations, the DC-DC converter has to maintain a stable output voltage. During the simulations only CCM operation is considered. It is worth noting that the proposed controller is capable to operate in Discontinuous Conduction Mode (DCM) with only a few extensions to the control architecture. This extensions include a zero crossing detection of the inductor current, a readjustment factor of the ramp coefficient and additional control logic to handle the DCM operation.

Fig. 6 shows a variation of the load current from 0.1 A to 0.6 A at time instant 5 µs. The first graph illustrates the transient of the output voltage v_{o} and the second graph the variation of the inductor current i_{L}. Fig. 7 shows the same graphs for a load variation from 0.6 A to 0.1 A at time instant 5 µs. The system has successfully reached the steady-state before applying the load steps. Fig. 8 depicts the maximum undershoot of the output voltage for different variations of the load current starting from a step of 100 mA up to 500 mA. The results of the simulations verify that the controller is able to effectively handle both, positive and negative variations in the applied load current. The output voltage v_{o} shows a tight regulation performance with a required regulation time of only a few µs. For the whole range of applied load variations the proposed digital sliding mode controller is able to achieve excellent regulation performance. Furthermore, the relation between undershoot and applied load step remains almost linear over the whole operation range.

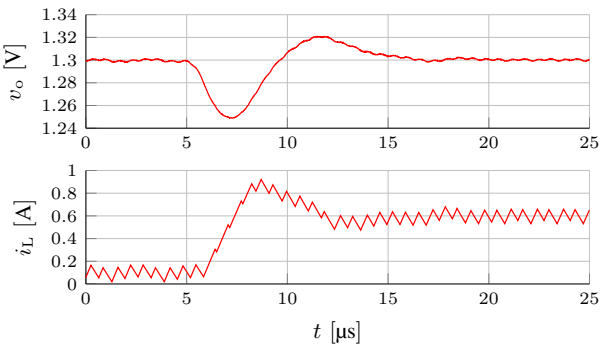

Fig. 6. Output voltage and inductor current waveforms of a Buck converter during a positive load transient from 0.1 A to 0.6 A.

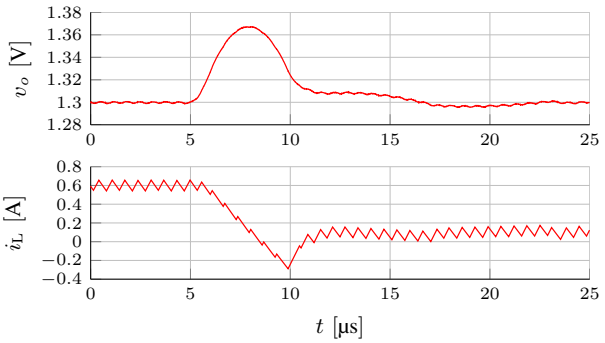

Fig. 7. Output voltage and inductor current waveforms of a Buck converter during a negative load transient from 0.6 A to 0.1 A.

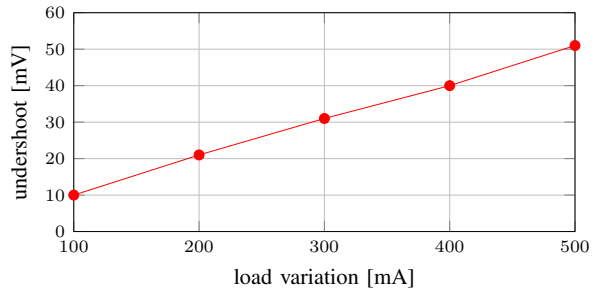

Fig. 8. Maximum undershoot of the output voltage transient for different variations of the load current.

It is worth noting that similar results can be achieved for the case of a Boost converter and also for DCM operation. Hence, the ability to control different converter topologies with a universal control structure can be exploited, for example, in a noninverting Buck-Boost converter, which can be operated either in Buck or Boost mode [1]. Furthermore, with a few extensions the proposed digital sliding mode controller is able to operate in both CCM and DCM. When switching modes no transient effects occur since the SMC is not based on a linearized model as conventional linear controllers.

V. Conclusions

A nonlinear control algorithm based on the theory of sliding mode control, with extensions in order to guarantee a constant switching frequency and to support different converter topologies and operating modes, has been proposed and discussed in this paper. An implementation in the digital domain has been presented and simulations have been shown for the case of a Buck converter operating in CCM. The proposed controller architecture is effectively capable of regulating the output voltage of the Buck converter with a tight dynamic performance and a small steady-state ripple.

Future work will focus on the development of an algorithm for the estimation of the inductor current and a hardware prototype to verify the simulation results.

References

[1] M. Agostinelli, R. Priewasser, S. Marsili, and M. Huemer, "Fixed-Frequency Pseudo Sliding Mode Control for a Buck-Boost DC-DC Converter in Mobile Applications: a Comparison with a Linear PID Controller," in *Proc. IEEE Intl. Symp. on Circuits and Syst. (ISCAS)*, May 2011, pp. 1604–1607.

[2] R. Priewasser, M. Agostinelli, S. Marsili, D. Straeussnigg, and M. Huemer, "Comparative study of linear and non-linear integrated control schemes applied to a Buck converter for mobile applications," *e&i Journal (Journal of the Austrian Eletcrotechnical Association, OVE)*, vol. 127, pp. 103–108, Apr. 2010.

[3] M. Agostinelli, R. Priewasser, S. Marsili, and M. Huemer, "Nonlinear control for energy efficient DC-DC converters supporting DCM operation," in *Proc. IEEE Intl. Midwest Symp. on Circuits and Syst. (MWSCAS)*, Aug. 2010, pp. 1153–1156.

[4] S.-C. Tan, Y. Lai, and C. Tse, "General Design Issues of Sliding-Mode Controllers in DC-DC Converters," *IEEE Trans. Ind. Electron.*, vol. 55, no. 3, pp. 1160 – 1174, Mar. 2008.

[5] "Special issue on digital control in power electronics," *IEEE Trans. Power Electron.*, vol. 18, no. 1, pp. 293–503, Jan. 2003.

[6] Y.-F. Liu, E. Meyer, and X. Liu, "Recent Developments in Digital Control Strategies for DC/DC Switching Power Converters," *IEEE Trans. Power Electron.*, vol. 24, no. 11, pp. 2567–2577, Nov. 2009.

[7] R. Priewasser, M. Agostinelli, S. Marsili, and M. Huemer, "Digital controller design for point-of-load DC-DC converters with variable switching frequency," *IET Electronics Letters*, vol. 47, no. 6, pp. 374 – 375, Mar. 2011.

[8] S.-C. Tan, Y. M. Lai, and C. K. Tse, "A unified approach to the PWM-based sliding-mode voltage controllers for basic DC-DC converters in continuous conduction mode," *IEEE Trans. Circuits Syst. I*, vol. 53, no. 8, pp. 1816–1827, Aug. 2006.

[9] V. Utkin, *Sliding Modes and Their Application in Variable Structure Systems*. MIR, 1978.

[10] V. Utkin, J. Guldner, and J. Shi, *Sliding Mode Control in Electromechanical Systems*. Taylor and Francis, 1999.

[11] R. Venkataramanan, "Sliding mode control of power converters," Ph.D. dissertation, California Institute of Technology, 1986.

[12] M. Agostinelli, R. Priewasser, S. Marsili, and M. Huemer, "Constant switching frequency techniques for sliding mode control in DC-DC converters," in *Proc. IEEE Intl. Symp. on Theoretical Electrical Engineering (ISTET)*, Klagenfurt, Austria, Jul. 2011, pp. 1–5.

[13] G. Spiazzi, P. Mattavelli, and L. Rossetto, "Sliding mode control of DC-DC converters," in *Proc. Brazilian Power Electron. Conf. (COBEP)*, Dec. 1997, pp. 59 – 68.

[14] H.-C. Lin and T.-Y. Chang, "Analysis and Design of a Sliding Mode Controller for Buck Converters Operating in DCM with Adaptive Hysteresis Band Control Scheme," *Intl. Conf. on Power Electron. and Drive Syst.*, pp. 372–377, Nov. 2007.

[15] A. Babazadeh and D. Maksimovic, "Hybrid Digital Adaptive Control for Fast Transient Response in Synchronous Buck DC-DC Converters," *IEEE Trans. Power Electron.*, vol. 24, no. 11, pp. 2625–2638, Nov. 2009.

[16] S.-C. Tan, Y. M. Lai, C. K. Tse, and M. K. H. Cheung, "A fixed-frequency pulsewidth modulation based quasi-sliding-mode controller for buck converters," *IEEE Trans. Power Electron.*, vol. 20, no. 6, pp. 1379–1392, Nov. 2005.

[17] J.-C. Olivier, J.-C. L. Claire, and L. Loron, "An Efficient Switching Frequency Limitation Process Applied to a High Dynamic Voltage Supply," *IEEE Trans. Power Electron.*, vol. 23, no. 1, pp. 153–162, Jan. 2008.

[18] A. Lachichi, S. Pierfederici, J.-P. Martin, and B. Davat, "Study of a Hybrid Fixed Frequency Current Controller Suitable for DC-DC Applications," *IEEE Trans. Power Electron.*, vol. 23, no. 3, pp. 1437–1448, May 2008.

[19] J. Ackermann and V. I. Utkin, "Sliding mode control design based on Ackermann's formula," *Proc. IEEE Conf. on Decision and Control*, vol. 4, pp. 3622–3627, Dec. 1994.

[20] R. Erickson and D. Maksimović, *Fundamentals of Power Electronics*, 2nd ed. Springer, 2001.

[21] Linear Technologies, *LTC3404: 1.4MHz High Efficiency Monolithic Synchronous Step-Down Regulator Datasheet*. [Online]. Available: http://cds.linear.com/docs/en/datasheet/3404fb.pdf